Canad. Math. Bull. Vol. **61** (3), 2018 pp. 518–530
http://dx.doi.org/10.4153/CMB-2017-072-x
©Canadian Mathematical Society 2018

Bounds on Multiple Self-avoiding Polygons

Kyungpyo Hong and Seungsang Oh

Abstract. A self-avoiding polygon is a lattice polygon consisting of a closed self-avoiding walk on a square lattice. Surprisingly little is known rigorously about the enumeration of self-avoiding polygons, although there are numerous conjectures that are believed to be true and strongly supported by numerical simulations. As an analogous problem to this study, we consider multiple self-avoiding polygons in a confined region as a model for multiple ring polymers in physics. We find rigorous lower and upper bounds for the number $p_{m\times n}$ of distinct multiple self-avoiding polygons in the $m \times n$ rectangular grid on the square lattice. For $m = 2$, $p_{2\times n} = 2^{n-1} - 1$. And for integers $m, n \geq 3$,

$$2^{m+n-3}\left(\tfrac{17}{10}\right)^{(m-2)(n-2)} \leq p_{m\times n} \leq 2^{m+n-3}\left(\tfrac{31}{16}\right)^{(m-2)(n-2)}.$$

1 Introduction

The enumeration of self-avoiding walks and polygons is one of the most important and classic combinatorial problems [3,10]. These were first introduced by the chemist Paul Flory [2] as models of polymers in dilute solution. The exact number of self-avoiding walks and polygons is still undetermined, although there are mathematically proven methods for approximating them.

A particularly interesting polygon model of a ring polymer with excluded volume is a lattice polygon that sits in a regular lattice, usually the two dimensional square lattice or the three dimensional cubic lattice. Here we consider the problem of self-avoiding polygons (SAP) on the square lattice $\mathbb{Z}^2$. Let p_n denote the number of distinct SAPs of length n, counted up to translational invariance on the square lattice $\mathbb{Z}^2$. Hammersley [4] proved that the number p_n grows exponentially: more precisely, the limit $\mu = \lim_{n\to\infty} p_{2n}^{1/2n}$ is known to exist. Furthermore, it is generally believed [10] that $p_{2n} \sim \mu^{2n} n^{\alpha-3}$ as $n \to \infty$. Here μ is called the *connective constant* of the lattice, and α is the *critical exponent.* The reader can find more details in [7].

In this paper, we are interested in another point of view of scaling arguments of multiple polygons on the square lattice, related to the size of a rectangle containing them instead of their length; see Figure 1. Let $\mathbb{Z}_{m\times n}$ denote the $m \times n$ rectangular grid on $\mathbb{Z}^2$, and let $p_{m\times n}$ be the number of distinct multiple self-avoiding polygons (MSAP) in $\mathbb{Z}_{m\times n}$. Here two MSAPs are considered to be different even though one can be translated upon the other. Note that in physics they serve as a model for multiple ring polymers in a confined region.

Received by the editors May 11, 2017; revised October 19, 2017.
Published electronically January 16, 2018.
Author S. O. (corresponding author) was supported by the National Research Foundation of Korea(NRF) grant, funded by the Korea government(MSIP) (No. NRF-2017R1A2B2007216).
AMS subject classification: **57M25**, 82B20, 82B41, 82D60.
Keywords: ring polymer, self-avoiding polygon.

https://doi.org/10.4153/CMB-2017-072-x Published online by Cambridge University Press

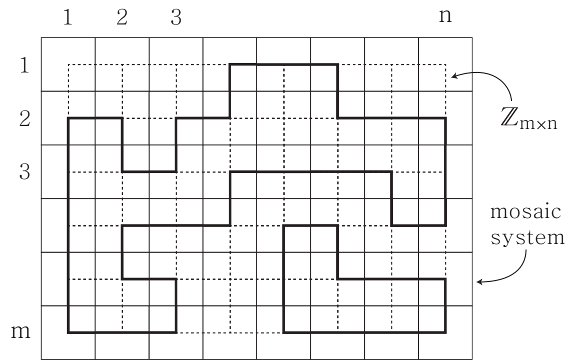

Figure 1: Two different viewpoints of an MSAP model in the confined square lattice $\mathbb{Z}_{m\times n}$ and in the mosaic system (explained in Section 2).

It is relatively easy to calculate that $p_{2\times n} = 2^{n-1} - 1$ for $m = 2$. But, for larger m, n of $p_{m\times n}$, the problem becomes increasingly difficult due to its non-Markovian nature. The main purpose of this paper is to establish rigorous lower and upper bounds for $p_{m\times n}$.

Theorem 1.1 *For integers $m, n \geq 3$,*

$$2^{m+n-3}\Big(\frac{17}{10}\Big)^{(m-2)(n-2)} \leq p_{m\times n} \leq 2^{m+n-3}\Big(\frac{31}{16}\Big)^{(m-2)(n-2)}.$$

Note that various types of single self-avoiding walks in a confined square lattice were investigated in [1], particularly a class of self-avoiding walks that start at the origin $(0,0)$, end at (n,n), and are entirely contained in the square $[0,n]\times[0,n]$ on $\mathbb{Z}^2$. The number of distinct walks is known to grow as $\lambda^{n^2+o(n^2)}$. They estimate $\lambda = 1.744550 \pm 0.000005$ as well as obtain strict upper and lower bounds, $1.628 < \lambda < 1.782$. In our model,

$$1.7 \leq \lim_{n\to\infty}(p_{n\times n})^{1/n^2} \leq 1.9375,$$

provided the limit exists.

2 Adjusting to the Mosaic System

A mosaic system was introduced by Lomonaco and Kauffman [9] to give a precise and workable definition of quantum knots. This definition is intended to represent an actual physical quantum system. The definition of quantum knot was based on the planar projections of knots and the Reidemeister moves. They model the topological information in a knot by a state vector in a Hilbert space that is directly constructed from knot mosaics. Recently Hong, Lee, Lee and Oh announced several results on the enumeration of various types of knot mosaics in the confined mosaic system in the series of papers [5, 6, 8, 11].

https://doi.org/10.4153/CMB-2017-072-x Published online by Cambridge University Press

We begin by explaining the basic notion of mosaics modified for polygons in $\mathbb{Z}_{m\times n}$. The following seven symbols are called *mosaic tiles* (for polygons). In the original definition in mosaic theory, there are eleven types of mosaic tiles, allowing four more mosaic tiles with two arcs.

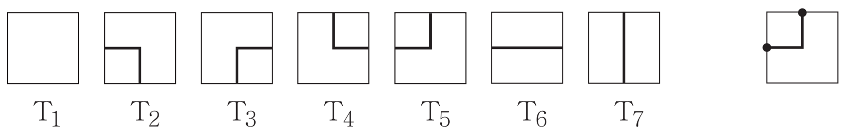

Figure 2: Seven mosaic tiles modified for polygons and connection points in a mosaic tile.

For positive integers m and n, an (m,n)*-mosaic* is an $m \times n$ matrix $M = (M_{ij})$ of mosaic tiles. The *trivial mosaic* is a mosaic whose entries are all T_1. A *connection point* of a mosaic tile is defined as the midpoint of a tile edge that is also the endpoint of a portion of graph drawn on the tile, as shown in the rightmost tile in Figure 2. Note that T_1 has no connection point and each of the six mosaic tiles T_2 through T_7 have two. A mosaic is called *suitably connected* if any pair of mosaic tiles lying immediately next to each other in either the same row or the same column have or do not have connection points simultaneously on their common edge. A *polygon* (m,n)*-mosaic* is a suitably connected (m,n)-mosaic that has no connection point on the boundary edges. Examples in Figure 3 are a non-polygon $(4,4)$-mosaic and a polygon $(4,4)$-mosaic.

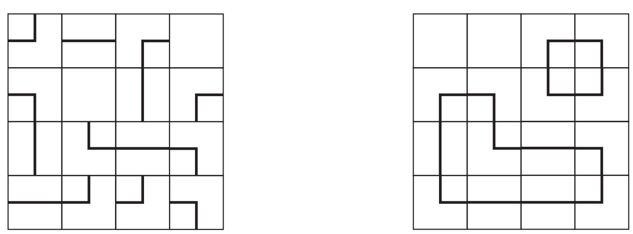

Figure 3: Examples of a non-polygon $(4,4)$-mosaic and a polygon $(4,4)$-mosaic

As drawn by solid line segments in Figure 1, we can consider a MSAP as a polygon (m,n)-mosaic by shifting the rectangular grid $\mathbb{Z}_{(m+1)\times(n+1)}$ horizontally and vertically by $-\frac{1}{2}$. In the mosaic system, polygons transpass unit length edges of the mosaic system and run through the centers of unit squares. The following one-to-one conversion arises naturally.

One-to-one conversion There is a one-to-one correspondence between MSAPs in $\mathbb{Z}_{m\times n}$ and polygon (m,n)-mosaics, except for the trivial mosaic.

Note that the trivial mosaic contains no graph, and so is not counted in $p_{m\times n}$.

https://doi.org/10.4153/CMB-2017-072-x Published online by Cambridge University Press

3 Quasimosaics and Growth Ratios

In this section, we define a modified version of quasimosaics, which were introduced in [6], and their growth ratios. We arrange all mosaic tiles as a sequence such that their pair-indices of tiles are ordered as $(1,1)$, $(1,2)$, $(2,1)$, $(1,3)$, $(2,2)$, $(3,1)$, etc., and finished at (m,n). More precisely, the pair-index (i,j) follows $(i-1,j+1)$ if $i>1$ and $j<n$, or otherwise, either $(i+j-2,1)$ for $i+j-2\le m$ or $(m,i+j-m-1)$ for $i+j-2>m$. Let $a(i,j)$ denote the predecessor of the pair-index (i,j) in the sequence.

An (i,j)-*quasimosaic* is a portion of a polygon (m,n)-mosaic obtained by taking all mosaic tiles $M_{1,1}$ through $M_{i,j}$ in the sequence as drawn in Figure 4. Note that a quasimosaic is also suitably connected. Its (i,j)-entry $M_{i,j}$ is called the *leading mosaic tile* of the (i,j)-quasimosaic. Furthermore we define two kinds of cling mosaics of the (i,j)-quasimosaic. An *l-cling mosaic* for $M_{i,j}$ is a submosaic consisting of three or fewer mosaic tiles $M_{i,j-2}$, $M_{i,j-1}$ and $M_{i+1,j-2}$ (they may not exist when $j=1$ or 2). And a *t-cling mosaic* is a submosaic consisting of five or fewer mosaic tiles $M_{i-2,j}$, $M_{i-2,j+1}$, $M_{i-2,j+2}$, $M_{i-1,j}$ and $M_{i-1,j+1}$. The letters l- and t- mean the left and the top, respectively. The leftmost and the top boundary edges of cling mosaics that are not contained in the boundary edges of the mosaic system are called *contact edges*.

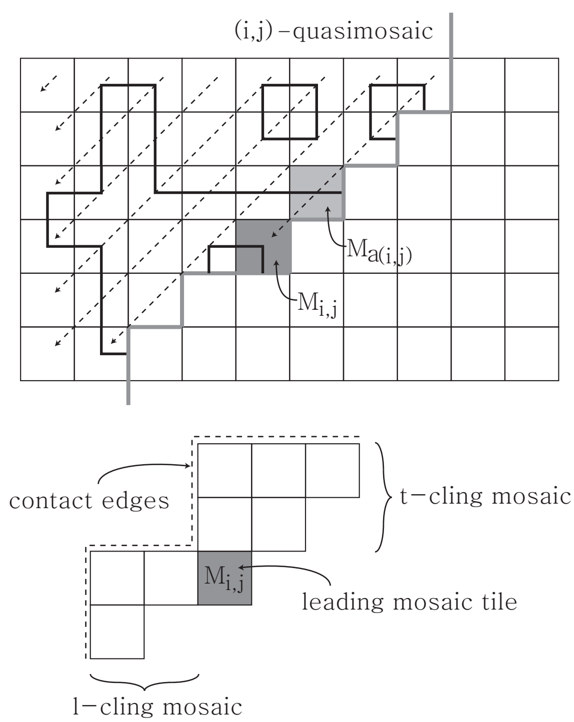

Figure 4: A $(4,5)$-quasimosaic and two cling mosaics.

https://doi.org/10.4153/CMB-2017-072-x Published online by Cambridge University Press

Let $Q_{i,j}$ denote the set of all possible (i,j)-quasimosaics. By definition, $Q_{m,n}$ is the set of all polygon (m,n)-mosaics. It is an exercise for the reader to show that $|Q_{1,1}| = 2$, $|Q_{1,2}| = 4$, $|Q_{2,1}| = 8$, $|Q_{1,3}| = 16$, $|Q_{2,2}| = 28$ and $|Q_{3,1}| = 56$, provided that $m, n \geq 4$. We will construct $Q_{m,n}$ from $Q_{1,1}$ by adding leading mosaic tiles inductively. Focus on the ratios of growth of the number of sets at each step. Define a *growth ratio* $r_{i,j}$ of the set $Q_{i,j}$ over $Q_{a(i,j)}$ as

$$r_{i,j} = \frac{|Q_{i,j}|}{|Q_{a(i,j)}|},$$

with the assumption that $|Q_{a(1,1)}| = 1$. Thus, $r_{1,1} = 2$, $r_{1,2} = 2$, $r_{2,1} = 2$, $r_{1,3} = 2$, $r_{2,2} = \frac{7}{4}$, and $r_{3,1} = 2$. By definition,

$$p_{m \times n} = |Q_{m,n}| - 1 = \prod_{i,j} r_{i,j} - 1. \tag{3.1}$$

For simplicity of exposition, a mosaic tile is called *l-cp* if it has a connection point on its left edge, and, similarly, t, r, or b-cp when on its top, right, or bottom edge, respectively. Sometimes we use two letters, for example, lt-cp in the case of both l-cp and t-cp. Also, we use the sign $\sim$ for negation, so that, for example, $\tilde{t}$-cp means not t-cp, $\tilde{l}\tilde{t}$-cp means both $\tilde{l}$-cp and $\tilde{t}$-cp, and $\widetilde{lt}$-cp (which is different from $\tilde{l}\tilde{t}$-cp) means not lt-cp, *i.e.,* $\tilde{l}t$, $l\tilde{t}$, or $\tilde{l}\tilde{t}$-cp.

Lemma 3.1 *For positive integers i, j, M_{ij} is either T_1 or T_3 if it is $\tilde{l}\tilde{t}$-cp, either T_2 or T_6 if $l\tilde{t}$-cp, either T_4 or T_7 if $\tilde{l}t$-cp, and T_5 if lt-cp. Therefore, each M_{ij} has two choices of mosaic tiles if it is $\widetilde{lt}$-cp, and the unique choice if it is lt-cp.*

Remark that we easily find rough bounds of $r_{i,j}$. Each $a(i,j)$-quasimosaic in $Q_{a(i,j)}$ can be extended to either one or two (i,j)-quasimosaics in $Q_{i,j}$ by choosing the leading mosaic tile $M_{i,j}$ being suitably connected according to Lemma 3.1. Thus, $|Q_{a(i,j)}| \leq |Q_{i,j}| \leq 2|Q_{a(i,j)}|$, and so we have rough bounds of the growth ratio:

$$1 \leq r_{i,j} \leq 2.$$

4 Investment of Cling Mosaics and cp-ratios

We can mark a mosaic tile edge on a cling mosaic with an 'x' if it does not have a connection point and with an 'o' if it has. Sometimes we use a sequence of x's and o's to mark several edges together, like $e_1 e_2 = $ xo, which means that the edge e_1 does not have a connection point but the edge e_2 does.

Now we classify all l-cling mosaics into five types $U_1 \sim U_5$, and all t-cling mosaics into eight types $V_1 \sim V_8$ as drawn in Figure 5. In each type, the bold edges e_l and e_t indicate the left and the top edges of the leading mosaic tile, respectively; the e_i's indicate the contact edges, and the edges marked by x lie in the boundary of the mosaic system (so these have no connection point). Note that the mosaic types other than U_1 and V_1 arise when the leading mosaic tile is near the boundary of the mosaic system.

Now we define cp-ratios for each type of cling mosaic as follows. We say that the associated contact edges e_i's are *given* if the presence of connection points of them are

https://doi.org/10.4153/CMB-2017-072-x Published online by Cambridge University Press

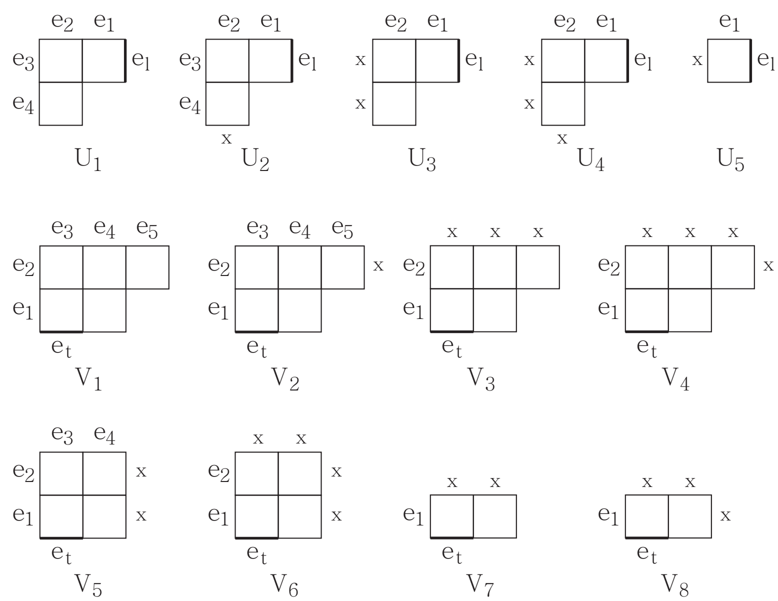

Figure 5: Five types of l-cling mosaics and eight types of t-cling mosaics

given. For a type U_k and given e_i's, we define

$$\textit{cp-ratio} \text{ of } U_k = \frac{|\{\text{type } U_k \text{ cling mosaics with the given } e_i\text{'s and } e_l = \text{o}\}|}{|\{\text{type } U_k \text{ cling mosaics with the given } e_i\text{'s and any } e_l\}|}.$$

And u_k denotes the pair of the minimum and the maximum among all cp-ratios for the type U_k that occur in any given e_i's. Similarly, define the pair $v_{k'}$ for the type $V_{k'}$.

Lemma 4.1 *The pairs of cp-ratios for the thirteen types of cling mosaics are as follows:* $u_1 = \{\frac{1}{4}, \frac{1}{2}\}$, $u_2 = u_3 = u_4 = v_5 = v_6 = \{\frac{1}{3}, \frac{1}{2}\}$, $v_1 = \{\frac{1}{4}, \frac{3}{5}\}$, $v_2 = \{\frac{1}{4}, \frac{4}{7}\}$, $v_3 = v_4 = \{\frac{4}{11}, \frac{1}{2}\}$, *and* $u_5 = v_7 = v_8 = \{\frac{1}{2}, \frac{1}{2}\}$.

Proof First, consider a submosaic W consisting of three mosaic tiles M_1, M_2, and M_3 as drawn in the center of Figure 6. Each of e_1e_2 and e_3e_4 has four choices of the presence of connection points among xx, xo, ox and oo. Define 4×4 matrices $N_{c_1c_2} = (n_{ij})$, where n_{ij} is the number of all possible suitably connected submosaics W with the given c_1c_2, the i-th e_1e_2 and the j-th e_3e_4 in the order of xx, xo, ox, and oo. Then

$$N_{\text{xx}} = \begin{bmatrix} 2 & 2 & 2 & 2 \\ 2 & 2 & 1 & 1 \\ 2 & 2 & 2 & 2 \\ 2 & 2 & 1 & 1 \end{bmatrix}, \; N_{\text{xo}} = \begin{bmatrix} 2 & 1 & 2 & 1 \\ 2 & 1 & 1 & 1 \\ 2 & 1 & 2 & 1 \\ 2 & 1 & 1 & 1 \end{bmatrix},$$

$$N_{\text{ox}} = \begin{bmatrix} 2 & 2 & 2 & 2 \\ 2 & 2 & 1 & 1 \\ 1 & 1 & 1 & 1 \\ 1 & 1 & 1 & 1 \end{bmatrix} \text{ and } N_{\text{oo}} = \begin{bmatrix} 2 & 1 & 2 & 1 \\ 2 & 1 & 1 & 1 \\ 1 & 1 & 1 & 0 \\ 1 & 0 & 1 & 1 \end{bmatrix}.$$

https://doi.org/10.4153/CMB-2017-072-x Published online by Cambridge University Press

These four matrices can be obtained from the following two rules. The first is that if e_2e_3 is oo, then M_3 is lt-cp, so it is uniquely determined by Lemma 3.1 and must be $\tilde{r}\tilde{b}$-cp. And if e_2e_3 is not oo, then M_3 is $\widetilde{lt}$-cp, so it has two choices of mosaic tiles for given e_2e_3, one of which is $\tilde{r}$-cp and the other is r-cp (similarly for b-cp). The second rule is that, after M_3 is determined, if M_3 is $\tilde{r}$-cp, then M_1 is uniquely determined for given c_1e_1. And if M_3 is r-cp, then M_1 is uniquely determined when c_1e_1 is not oo, but there is no choice for M_1 when c_1e_1 is oo. The second rule can be applied to M_2 with c_2e_4 in the same manner.

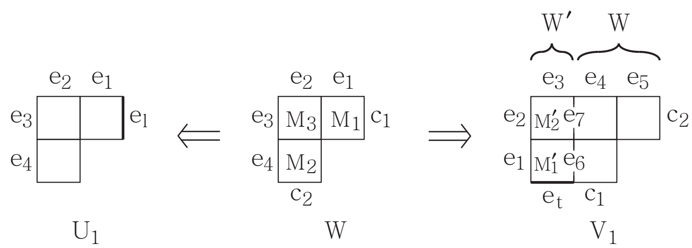

Figure 6: Submosaic W and modifying W to U_1 and V_1

For same sized matrices A and B, $\{\frac{A}{B}\}$ denotes the pair consisting of the minimum and the maximum among all entries of the matrix obtained from dividing A by B entry-wise. From now on, the mark $*$ is used when we consider both x and o. For example, $N_{O*} = N_{OX} + N_{OO}$.

For the types U_1 through U_4, we use W after identifying $c_1 = e_l$. Each entry of N_{O*} indicates the number of all possible type U_1 cling mosaics with given e_i's and $e_l = $ o, and N_{**} the number of type U_1 cling mosaics with given e_i's and any e_l. Note that there is no restriction on c_2. Thus, each entry of the matrix obtained from dividing N_{O*} by N_{**} entry-wise is the cp-ratio for given e_i's. Now u_1 is the pair of the minimum and the maximum among all entries of this matrix. Thus, $u_1 = \{\frac{N_{O*}}{N_{**}}\} = \{\frac{1}{4}, \frac{1}{2}\}$. u_2 can be obtained by merely changing N_{O*} and N_{**} by N_{OX} and N_{*X}, respectively, because $c_2 = $ x. Thus, $u_2 = \{\frac{N_{OX}}{N_{*X}}\} = \{\frac{1}{3}, \frac{1}{2}\}$.

The restriction $e_3e_4 = $ xx for the types U_3 and U_4 is related to only the first columns of the associated matrices. The rest of the proof is similar to the previous case. Thus,

$$u_3 = \left\{\frac{\text{1st column of } N_{O*}}{\text{1st column of } N_{**}}\right\} = \left\{\frac{1}{3}, \frac{1}{2}\right\} \quad \text{and} \quad u_4 = \left\{\frac{\text{1st column of } N_{OX}}{\text{1st column of } N_{*X}}\right\} = \left\{\frac{1}{3}, \frac{1}{2}\right\}.$$

For the types V_1 through V_4, we use W again after identifying e_1, e_2, e_3, and e_4 of W with e_6, e_7, e_4, and e_5 of the V_i's, respectively, combined with another submosaic W' as shown in Figure 6. Define two 4×8 matrices $N^{(1)}_{e_t} = (n_{ij})$, for $e_t = $ x or o, where n_{ij} is the number of all possible submosaics V_1 with the given e_t, the i-th e_1e_2 and the j-th $e_3e_4e_5$ in the reverse dictionary order as before. In the following matrices, "x-th row" and "$x + y$-th rows" mean the x-th row of the previously obtained matrix N_{**}

and the sum of the x-th row and the y-th row of N_{**}, respectively. Then

$$N_{\mathrm{x}}^{(1)} = \begin{bmatrix} 1{+}4\text{th rows} & 2{+}3\text{rd rows} \\ 2{+}3\text{rd rows} & 1\text{st row} \\ 2{+}3\text{rd rows} & 1{+}4\text{th rows} \\ 1{+}4\text{th rows} & 3\text{rd row} \end{bmatrix} = \begin{bmatrix} 14 & 10 & 12 & 10 & 14 & 11 & 10 & 8 \\ 14 & 11 & 10 & 8 & 8 & 6 & 8 & 6 \\ 14 & 11 & 10 & 8 & 14 & 10 & 12 & 10 \\ 14 & 10 & 12 & 10 & 6 & 5 & 6 & 4 \end{bmatrix},$$

$$N_{\mathrm{o}}^{(1)} = \begin{bmatrix} 2+3\text{rd rows} & 1+4\text{th rows} \\ 1+4\text{th rows} & 3\text{rd row} \\ 1\text{st row} & 2\text{nd row} \\ 2\text{nd row} & 1\text{st row} \end{bmatrix} = \begin{bmatrix} 14 & 11 & 10 & 8 & 14 & 10 & 12 & 10 \\ 14 & 10 & 12 & 10 & 6 & 5 & 6 & 4 \\ 8 & 6 & 8 & 6 & 8 & 6 & 4 & 4 \\ 8 & 6 & 4 & 4 & 8 & 6 & 8 & 6 \end{bmatrix}.$$

For example, we will compute the second row of $N_{\mathrm{x}}^{(1)}$, and the reader can find the remaining rows in the same manner. For this case, $e_t = \mathrm{x}$, $e_1e_2 = \mathrm{xo}$, the left four entries of this row are related to $e_3 = \mathrm{x}$, and the right four entries are related to $e_3 = \mathrm{o}$. If $e_3 = \mathrm{x}$, then the pair M_1' and M_2' of W' has two choices, such as $M_1' = T_1$ and $M_2' = T_6$, or $M_1' = T_4$ and $M_2' = T_2$. Therefore e_6e_7 must be xo or ox, respectively. These two cases are related to the second and the third rows of N_{**}, respectively. Thus the numbers of all possible such W for each e_4e_5 are represented by the sum of these two rows. If $e_3 = \mathrm{o}$, then this pair has the unique choice $M_1' = T_1$ and $M_2' = T_5$, and so e_6e_7 must be xx. It is related to the first row of N_{**}, which represents the numbers of all such W for each e_4e_5. Each entry of $N_{\mathrm{o}}^{(1)}$ indicates the number of all possible type V_1 t-cling mosaics with given e_i's and $e_t = \mathrm{o}$, and $N_*^{(1)}$ the number of type V_1 t-cling mosaics with given e_i's and any e_t. Now we get the cp-ratio for given e_i's in the same way as previously. Thus,

$$v_1 = \left\{ \frac{N_{\mathrm{o}}^{(1)}}{N_*^{(1)}} \right\} = \left\{ \frac{1}{4}, \frac{3}{5} \right\}.$$

For V_2, define other two 4×8 matrices $N_{e_t}^{(2)}$, for $e_t = \mathrm{x}$ or o. $N_{\mathrm{x}}^{(2)}$ and $N_{\mathrm{o}}^{(2)}$ are obtained in the same manner as computing $N_{\mathrm{x}}^{(1)}$ and $N_{\mathrm{o}}^{(1)}$ after replacing N_{**} by $N_{*\mathrm{x}}$, since $c_2 = \mathrm{x}$. Then

$$N_{\mathrm{x}}^{(2)} = \begin{bmatrix} 7 & 7 & 6 & 6 & 7 & 7 & 5 & 5 \\ 7 & 7 & 5 & 5 & 4 & 4 & 4 & 4 \\ 7 & 7 & 5 & 5 & 7 & 7 & 6 & 6 \\ 7 & 7 & 6 & 6 & 3 & 3 & 3 & 3 \end{bmatrix}, \quad N_{\mathrm{o}}^{(2)} = \begin{bmatrix} 7 & 7 & 5 & 5 & 7 & 7 & 6 & 6 \\ 7 & 7 & 6 & 6 & 3 & 3 & 3 & 3 \\ 4 & 4 & 4 & 4 & 4 & 4 & 2 & 2 \\ 4 & 4 & 2 & 2 & 4 & 4 & 4 & 4 \end{bmatrix}.$$

Then v_2 can be obtained from merely changing $N_{\mathrm{o}}^{(1)}$ and $N_*^{(1)}$ by $N_{\mathrm{o}}^{(2)}$ and $N_*^{(2)}$, respectively. Thus,

$$v_2 = \left\{ \frac{N_{\mathrm{o}}^{(2)}}{N_*^{(2)}} \right\} = \left\{ \frac{1}{4}, \frac{4}{7} \right\}.$$

The restriction $e_3e_4e_5 = \mathrm{xxx}$ for the types V_3 and V_4 is related to only the first columns of the associated matrices. Thus

$$v_3 = \left\{ \frac{\text{1st column of } N_{\mathrm{o}}^{(1)}}{\text{1st column of } N_*^{(1)}} \right\} = \left\{ \frac{4}{11}, \frac{1}{2} \right\} \quad \text{and} \quad v_4 = \left\{ \frac{\text{1st column of } N_{\mathrm{o}}^{(2)}}{\text{1st column of } N_*^{(2)}} \right\} = \left\{ \frac{4}{11}, \frac{1}{2} \right\}.$$

Consider the types V_5 and V_6. Define two 4×4 matrices $N_{e_t}^{(3)} = (n_{ij})$, for $e_t = \mathrm{x}$ or o, where n_{ij} is the number of all possible submosaics V_5 with the given e_t, the i-th e_1e_2,

https://doi.org/10.4153/CMB-2017-072-x Published online by Cambridge University Press

and the j-th e_3e_4. Using the same manner of computing the associated matrices at the beginning of the proof, the reader can find the matrices $N_{\mathrm{x}}^{(3)}$ and $N_{\mathrm{o}}^{(3)}$ as follows:

$$N_{\mathrm{x}}^{(3)} = \begin{bmatrix} 2 & 2 & 2 & 2 \\ 2 & 2 & 1 & 1 \\ 2 & 2 & 2 & 2 \\ 2 & 2 & 1 & 1 \end{bmatrix} \quad \text{and} \quad N_{\mathrm{o}}^{(3)} = \begin{bmatrix} 2 & 2 & 2 & 2 \\ 2 & 2 & 1 & 1 \\ 1 & 1 & 1 & 1 \\ 1 & 1 & 1 & 1 \end{bmatrix}.$$

From the same calculation as before,

$$v_5 = \left\{ \frac{N_{\mathrm{o}}^{(3)}}{N_*^{(3)}} \right\} = \left\{ \frac{1}{3}, \frac{1}{2} \right\} \quad \text{and} \quad v_6 = \left\{ \frac{\text{1st column of } N_{\mathrm{o}}^{(3)}}{\text{1st column of } N_*^{(3)}} \right\} = \left\{ \frac{1}{3}, \frac{1}{2} \right\}.$$

For the remaining types, u_5, v_7, and v_8 are obtained by counting directly for each case of $e_1 = \mathrm{x}$ or o, as $u_5 = v_7 = v_8 = \{\frac{1}{2}, \frac{1}{2}\}$. ■

5 Proof of Theorem 1.1

We will compute lower and upper bounds of the growth ratio at each leading mosaic tile by using the cp-ratios of the associated cling mosaics. Let $M_{i,j}$ be a leading mosaic tile with the associated l- and t-cling mosaics U_k and $V_{k'}$. Let $S_{kk'}$ and $L_{kk'}$ denote the multiplication of the smallest (resp. largest) elements of u_k and $v_{k'}$.

Lemma 5.1 *For $i \neq 1, m$ and $j \neq 1, n$, $2 - L_{kk'} \le r_{ij} \le 2 - S_{kk'}$.*

Proof Suppose that $i \neq 1, m$ and $j \neq 1, n$. Recall that an (i, j)-quasimosaic in $Q_{i,j}$ is obtained from a $a(i, j)$-quasimosaic in $Q_{a(i,j)}$ by attaching a proper leading mosaic tile $M_{i,j}$. This mosaic tile should be suitably connected according to the presence of connection points on its left and top edges. In this stage, there are two possibilities, as follows: if $M_{i,j}$ is $\widetilde{lt}$-cp, then it has two choices, and if it is lt-cp, then it has a unique choice. Therefore, for given cling mosaics, $M_{i,j}$ has a unique choice only when $e_l e_t =$ oo.

Consider a submosaic consisting of $M_{i,j}$ and l- and t-cling mosaics. Assume that the presence of connection points on all contact edges e_i's are given. Then

$$\frac{|\{(i,j)\text{-quasimosaics with the given } e_i\text{'s}\}|}{|\{a(i,j)\text{-quasimosaics with the given } e_i\text{'s}\}|} = \frac{|\{\text{submosaics consisting of } M_{i,j} \text{ and the a.c.m.'s with the given } e_i\text{'s}\}|}{|\{\text{submosaics consisting of only the a.c.m.'s with the given } e_i\text{'s}\}|},$$

where a.c.m. means associated cling mosaic.

Let c_k and $c'_{k'}$ denote the associated cp-ratios of the l- and t-cling mosaics for the given contact edges e_i's. Then the latter quotient of the equality is $2 \times (1 - c_k c'_{k'}) + 1 \times (c_k c'_{k'}) = 2 - c_k c'_{k'}$. Furthermore, $2 - c_k c'_{k'}$ must lie between $2 - L_{kk'}$ and $2 - S_{kk'}$, and hence, so does the former quotient. Therefore, r_{ij} lies between $2 - L_{kk'}$ and $2 - S_{kk'}$. ■

https://doi.org/10.4153/CMB-2017-072-x Published online by Cambridge University Press

Lemma 5.2 *Let m and n be integers with* $3 \le m \le n$.

For $m = 3$, $\quad 14\left(\frac{7}{2}\right)^{n-3} - 1 \le p_{3\times n} \le 14\left(\frac{11}{3}\right)^{n-3} - 1.$

For $m = 4$, $\quad 8\left(\frac{49}{8}\right)^{n-2} - 1 \le p_{4\times n} \le \frac{9520}{27}\left(\frac{155}{22}\right)^{n-4} - 1.$

For $m \ge 5$, $\quad 8\cdot 6^{m-4}\left(\frac{49}{8}\right)^{n-2}\left(\frac{17}{10}\right)^{(m-4)(n-4)} - 1 \le p_{m\times n},$

$$p_{m\times n} \le \frac{337280}{1863}\left(\frac{2645}{192}\right)^{m-4}\left(\frac{2415}{176}\right)^{n-4}\left(\frac{31}{16}\right)^{(m-5)(n-5)} - 1.$$

Proof First we handle the general case that $5 \le m < n$. Consider a leading mosaic tile $M_{i,j}$ for $4 \le i \le m-2$ and $4 \le j \le n-3$. Associated l- and t-cling mosaics are of types U_1 and V_1, respectively, because they are apart from the boundary of the mosaic system. Since the smallest cp-ratios in u_1 and v_1 are both $\frac{1}{4}$ and their largest cp-ratios are $\frac{1}{2}$ and $\frac{3}{5}$, respectively, r_{ij} lies between $2 - L_{11} = \frac{17}{10}$ and $2 - S_{11} = \frac{31}{16}$. For the remaining leading mosaic tiles, one or both of their associated cling mosaics are attached to the boundary of the mosaic system.

A chart in Figure 7, called the *cling mosaic chart*, illustrates all possible combinations of cling mosaics at each position of leading mosaic tile. For example, at the position of the leading mosaic tile $M_{3,2}$, the associated l- and t-cling mosaics are of types U_5 and V_3, respectively.

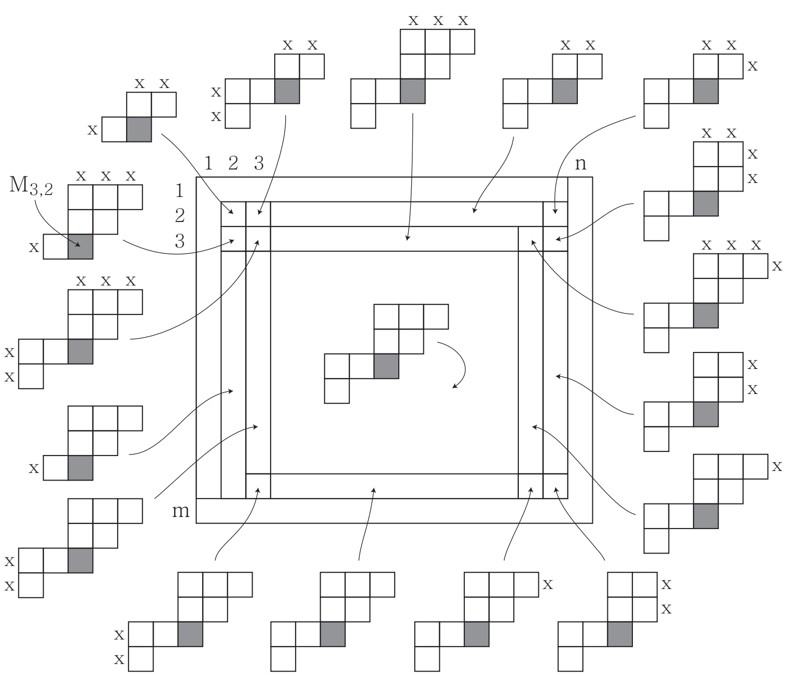

Figure 7: Cling mosaic chart for the general case.

https://doi.org/10.4153/CMB-2017-072-x Published online by Cambridge University Press

From Lemmas 4.1 and 5.1 combined with the cling mosaic chart, we get Table 1, called the *growth ratio table*. Each row explains the placements of leading mosaic tiles $M_{i,j}$, the associated multiplications $u_k \cdot v_{k'}$ of cp-ratios, possible variance of the related growth ratios $r_{i,j}$, and the number of related mosaic tiles.

Note that for $i = 1$ $(j \neq n)$, the leading mosaic tile $M_{1,j}$ must be $\tilde{t}$-cp. Assume that $M_{1,j-1}$ is already decided. Then $M_{1,j}$ has exactly two choices by Lemma 3.1, so $r_{1j} = 2$. Similarly, we get $r_{i1} = 2$ for $j = 1$ $(i \neq m)$. And for $i = m$, $M_{m,j}$ must be $\tilde{b}$-cp. Assume that $M_{m,j-1}$ and $M_{m-1,j}$ are already decided. But in any case, $M_{m,j}$ is determined uniquely, so $r_{mj} = 1$. Similarly, we get $r_{in} = 1$ for $j = n$. Indeed, the method in this paragraph works for all the cases of $3 \leq m \leq n$.

(i,j) of $M_{i,j}$	$u_k \cdot v_{k'}$	$r_{i,j}$	*number of tiles*
$i = 1$ or $j = 1$ except $(1,n),(m,1)$		2	$m+n-3$
$i = m$ or $j = n$		1	$m+n-1$
$4 \leq i \leq m-2$ and $4 \leq j \leq n-3$	$u_1 \cdot v_1$	$\frac{17}{10} \sim \frac{31}{16}$	$(m-5)(n-6)$
$(2,2)$	$u_5 \cdot v_7$	$\frac{7}{4}$	1
$(2,3)$	$u_3 \cdot v_7$	$\frac{7}{4} \sim \frac{11}{6}$	1
$i = 2$ and $4 \leq j \leq n-2$	$u_1 \cdot v_7$	$\frac{7}{4} \sim \frac{15}{8}$	$n-5$
$(2,n-1)$	$u_1 \cdot v_8$	$\frac{7}{4} \sim \frac{15}{8}$	1
$(3,2)$	$u_5 \cdot v_3$	$\frac{7}{4} \sim \frac{20}{11}$	1
$(3,3)$	$u_3 \cdot v_3$	$\frac{7}{4} \sim \frac{62}{33}$	1
$i = 3$ and $4 \leq j \leq n-3$	$u_1 \cdot v_3$	$\frac{7}{4} \sim \frac{21}{11}$	$n-6$
$(3,n-2)$	$u_1 \cdot v_4$	$\frac{7}{4} \sim \frac{21}{11}$	1
$(3,n-1)$	$u_1 \cdot v_6$	$\frac{7}{4} \sim \frac{23}{12}$	1
$4 \leq i \leq m-1$ and $j = 2$	$u_5 \cdot v_1$	$\frac{17}{10} \sim \frac{15}{8}$	$m-4$
$4 \leq i \leq m-2$ and $j = 3$	$u_3 \cdot v_1$	$\frac{17}{10} \sim \frac{23}{12}$	$m-5$
$4 \leq i \leq m-2$ and $j = n-2$	$u_1 \cdot v_2$	$\frac{12}{7} \sim \frac{31}{16}$	$m-5$
$4 \leq i \leq m-2$ and $j = n-1$	$u_1 \cdot v_5$	$\frac{7}{4} \sim \frac{23}{12}$	$m-5$
$(m-1,3)$	$u_4 \cdot v_1$	$\frac{17}{10} \sim \frac{23}{12}$	1
$i = m-1$ and $4 \leq j \leq n-3$	$u_2 \cdot v_1$	$\frac{17}{10} \sim \frac{23}{12}$	$n-6$
$(m-1,n-2)$	$u_2 \cdot v_2$	$\frac{12}{7} \sim \frac{23}{12}$	1
$(m-1,n-1)$	$u_2 \cdot v_5$	$\frac{7}{4} \sim \frac{17}{9}$	1

Table 1: Growth ratio table for the general case.

The chart in Figure 8 illustrates bounds of the growth ratios at each place of leading mosaic tile according to the growth ratio table. This is called the *growth ratio chart*.

https://doi.org/10.4153/CMB-2017-072-x Published online by Cambridge University Press

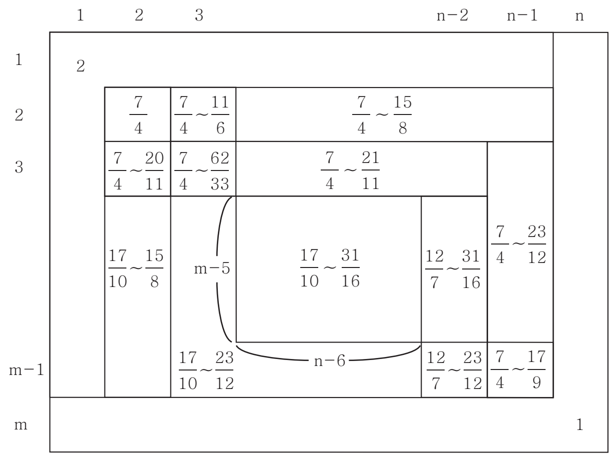

Figure 8: Growth ratio chart for the general case

From the growth ratio chart for $5 \le m < n$, we get rigorous lower and upper bounds for $p_{m\times n}$, which are obtained by merely multiplying every growth ratio at each leading mosaic tile and subtracting by 1 as in equation (3.1). Thus, we have

$$8 \cdot 6^{m-4}\left(\tfrac{49}{8}\right)^{n-2}\left(\tfrac{17}{10}\right)^{(m-4)(n-4)} - 1 \le p_{m\times n},$$

$$p_{m\times n} \le \frac{337280}{1863}\left(\tfrac{2645}{192}\right)^{m-4}\left(\tfrac{2415}{176}\right)^{n-4}\left(\tfrac{31}{16}\right)^{(m-5)(n-5)} - 1.$$

For the remaining cases $m = 3$, $m = 4$, and $m = n = 5$, the reader may draw the associated cling mosaic charts and compute the growth ratio tables. Then the related growth ratio charts will be obtained as shown in Figure 9. Furthermore,

$$14\left(\tfrac{7}{2}\right)^{n-3} - 1 \le p_{3\times n} \le 14\left(\tfrac{11}{3}\right)^{n-3} - 1 \qquad \text{for } m = 3, \text{ and}$$

$$8\left(\tfrac{49}{8}\right)^{n-2} - 1 \le p_{4\times n} \le \tfrac{9520}{27}\left(\tfrac{155}{22}\right)^{n-4} - 1 \qquad \text{for } m = 4.$$

Indeed for the case of $m = n = 5$, we eventually get the same result as in the general case, by applying $m = n = 5$. ■

Proof of Theorem 1.1 The result follows directly from Lemma 5.2 after loosening the bounds slightly. Speaking precisely, for any case of $3 \le m \le n$, if $i \ne 1, m$ and $j \ne 1, n$, then r_{ij} always lies between $\frac{17}{10}$ and $\frac{31}{16}$. Furthermore, if $i = 1$ or $j = 1$, except $(1, n)$ and $(m, 1)$, then $r_{ij} = 2$, and if $i = m$ or $j = n$, then $r_{ij} = 1$. Therefore,

$$2^{m+n-3}\left(\tfrac{17}{10}\right)^{(m-2)(n-2)} - 1 \le p_{m\times n} \le 2^{m+n-3}\left(\tfrac{31}{16}\right)^{(m-2)(n-2)} - 1.$$

Note that −1 can be ignored for the brief formula, since this inequality is obtained from Lemma 5.2 after loosening the bounds slightly. ■

https://doi.org/10.4153/CMB-2017-072-x Published online by Cambridge University Press

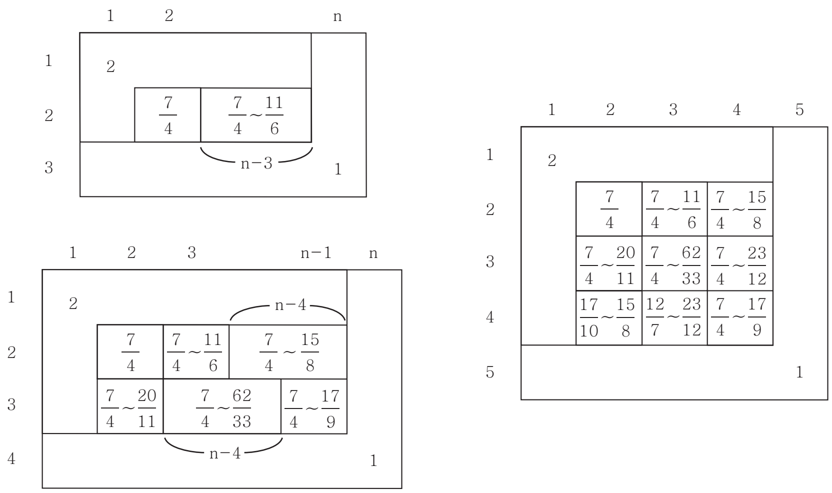

Figure 9: Three growth ratio charts for $m = 3$, $m = 4$, and $m = n = 5$ from the top left to the right

References

[1] M. Bousquet-Mélou, A. Guttmann, and I. Jensen, *Self-avoiding walks crossing a square*. J. Phys. A **38**(2005), no. 42, 9159–9181. http://dx.doi.org/10.1088/0305-4470/38/42/001

[2] P. Flory, *The configuration of real polymer chains*. J. Chem. Phys. **17**(1949), 303–310.

[3] A. Guttmann, ed., *Polygons, polyominos, and polycubes*. Lecture Notes in Physics, 775, Springer, Dordrecht, 2009. http://dx.doi.org/10.1007/978-1-4020-9927-4

[4] J. M. Hammersley, *The number of polygons on a lattice*. Proc. Cambridge Philos. Soc. **57**(1961), 516–523.

[5] K. Hong, H. Lee, H. J. Lee, and S. Oh, *Upper bound on the total number of knot n-mosaics*. J. Knot Theory Ramifications **23**(2014), no. 13, 1450065. http://dx.doi.org/10.1142/S0218216514500655

[6] ———, *Small knot mosaics and partition matrices*. J. Phys. A **47**(2014), no. 43, 435201. http://dx.doi.org/10.1088/1751-8113/47/43/435201

[7] E. Janse van Rensburg, *Thoughts on lattice knot statistics*. J. Math. Chem. **45**(2009), no. 1, 7–38. http://dx.doi.org/10.1007/s10910-008-9364-9

[8] H. J. Lee, K. Hong, H. Lee, and S. Oh, *Mosaic number of knots*. J. Knot Theory Ramifications **23**(2014), no. 13, 1450069. http://dx.doi.org/10.1142/S0218216514500692

[9] S. Lomonaco and L. Kauffman, *Quantum knots and mosaics*. Quantum Inf. Process. **7**(2008), no. 2–3, 85–115. http://dx.doi.org/10.1007/s11128-008-0076-7

[10] N. Madras and G. Slade, *The Self-avoiding walk. Probability and its applications.* Birkhäuser Boston, Boston, MA, 1993.

[11] S. Oh, K. Hong, H. Lee, and H. J. Lee, *Quantum knots and the number of knot mosaics*. Quantum Inf. Process. **14**(2015), no. 3, 801–811. http://dx.doi.org/10.1007/s11128-014-0895-7

National Institute for Mathematical Sciences, Daejeon 34047, Korea
e-mail: kphong@nims.re.kr

Department of Mathematics, Korea University, Seoul 02841, Korea
e-mail: seungsang@korea.ac.kr

https://doi.org/10.4153/CMB-2017-072-x Published online by Cambridge University Press